# Ultra Wideband Power Divider Design Implementing Microstrip with Slotted Ground

**Norhudah Seman [1*], Khairul H. Yusof [2], Mohd H. Jamaluddin [1], and Tharek A. Rahman [1]**

[1] Wireless Communication Centre, School of Electrical Engineering
University Teknologi Malaysia, 81310 UTM Johor Bahru, Johor, Malaysia
huda@fke.utm.my, haizal@fke.utm.my, tharek@fke.utm.my

[2] Faculty of Engineering and Information Technology, MAHSA University
42610 Jenjarom, Selangor, Malaysia
khairulhuda@mahsa.edu.my

***Abstract*** ─ This article proposes a compact design of a two-section power divider, which operates over an ultra wideband frequency range of 3-11 GHz. The design approach of microtrip with slotline at the ground plane is applied to reduce the size of the circuit and to achieve wide bandwidth coverage. The rectangular slots are implemented at the ground plane, which is positioned symmetrically underneath the second and third arms of each microstrip quarter-wave transformer to reduce its length up to 33.34%. These attributes lead to an easily fabricated 20 mm x 23 mm compact power divider with a reduced size (by 23.33%). The bandwidth performance is improved up to 19.4% compared to a conventional divider. The design is realized by implementing the Rogers TMM4 substrate and simulated by using CST Microwave Studio. The power divider is verified by using a vector network analyzer (VNA). A good agreement between simulation and fabrication is achieved in terms of return loss, isolation and transmission coefficients across the UWB frequency range.

***Index Terms*** ─ Microstrip-slot, power divider, two-section, ultra wideband.

## I. INTRODUCTION

Nowadays, the general public desires faster mobile internet access, the latest communication gadgets, and unlimited communication and access to information. To date, avant-garde smartphones and tablets continue growing in demand, requiring more innovative multimedia capabilities. Consequently, the forthcoming fifth generation (5G) of wireless technology, which is presumed to arrive by 2020, is extensively studied. This future technology of 5G is expected to offer extremely high capacity and countless connections of billions of wireless gadgets with very low latency and response times. Hence, a massive multiple-input and multiple-output (MIMO) and distributed antenna system (DAS) technology are proposed for the respective indoor and outdoor applications of 5G architecture. These two approaches seem to be appropriate solutions for offering services with high data rates and quality [1]. In addition, to supporting for this requirement, various extensive research works are needed in component designs, including an alternative to a mixer as one of the important components in the wireless communication system. Commonly, a mixer consists of active devices that require a certain biasing circuit that leads to additional thorough design effort and complexity. Thus, a six-port network can be used as an alternative to the mixer-based approach. In contrast to the mixer, this six-port network can be formed by using only passive devices, such as a coupler, H-hybrid and power divider. Therefore, by having this network in the wireless communication system architecture, the complexity of the design can be reduced and, consequently, can increase the performance of the bandwidth.

The power divider is one of the important components in a six-port network, which requires a lot of effort to increase the bandwidth. One method has been introduced [2] that implements a multilayer technique formed by a microstrip-to-slot-to-microstrip transition. The design shows that the UWB operating frequency range from 3.1 to 10.6 GHz is achieved; however, the performance levels are degraded due to misalignment problems and the existence of an air gap between the two substrates [3]. Another method for achieving the desired wideband performance entails the use of a multi-section power divider [4]. To enhance the bandwidth performance and reduce the size of the circuit in a multi-section power divider design, a few other methods are added, such as compensation circuit [5], coupled line [6], combination of a coupled line and quasi-lumped element [7], least squares method [8], stub [9-11] and additional capacitance and inductance element [12].

*Submitted On: July 7, 2018*
*Accepted On: December 25, 2018*

Guo et al. proposed a novel design of a power divider, in which a coax balun transformer is used to replace the isolating resistor between the two output ports [5]. This technique increases the simulated bandwidth performance coverage from 490 to 830 MHz. However, the use of the coax balun transformer and dummy load in the proposed design leads to difficulty and complexity in the circuit design. In [6], a two-section coupled-line coupler at each of the quarter-wave transformer was proposed. The isolation performance of this design was improved up to 40 dB. However, the performance was limited to the narrowband frequency range. To overcome the bandwidth limitation by the design that was introduced in [6], Gruszczynski et al. proposed the quasi-lumped element technique for a multi-section coupled-line Wilkinson power divider design [7]. The structure is composed of a three-section coupled line with a quasi-lumped element approach. A wideband frequency response of 0.6 to 2.5 GHz and a small size circuit were achieved. However, to obtain the highest self-inductance per unit length, the width of the coupled strip at each coupled-line section had to be as narrow as possible to provide the shortest length of the coupled lines, which led to difficulties in the fabrication process. Meanwhile, in [8], Oraizi and Sharifi introduced a design and optimization procedure based on the method of least squares (MLS) for a multi-section Wilkinson power divider. The significant parts of the proposed method and design were that the performance of the phase difference between the two output ports operated well in a designated frequency band and that a minimization of the insertion loss could be incorporated into the expression of the error function. However, the performance was too narrow, which cover only 0.5-2.5 GHz.

The proposed power dividers in [9-11] utilized open-circuited stub on each branch in the designs. Design in [9] and [11] demonstrated good UWB performance from 3.1 to 10.6 GHz with well transmission coefficients, return losses and isolation. In contrast to [9, 11], design in [10] exhibited narrowband performance. Another UWB power divider reported in [12] was constructed using two sections of a four-way Wilkinson power divider, with one input port and four output ports. In addition to good UWB performance, band rejection was achieved in the design by using a symmetric spiral defect ground-slotted (DGS) structure. Even though [9, 12] offer UWB operation, the methods used has produced larger size circuits compared to the conventional two-section power divider. While [11] has compact size but its resistors that positioned further apart from the transmission may lead to fabrication difficulty.

Hence in this article, a new compact two-section UWB power divider formed by a microstrip-slot is proposed. By implementing this technique, a compact size of the power divider circuit with excellent ultra wideband performance from 3 to 11 GHz is achieved. The use of the microstrip slot in the design leads to the reduction of the quarter-wave transformer length of the power divider up to 33.34%, which consequently results in a reduced-size circuit. The initial dimension was calculated by using mathematical equations, as described in [4], which were obtained by using even- and odd-mode analysis. The design of the two-section power divider utilized a Rogers TMM4 substrate with the following features: 0.508 mm thickness, a dielectric constant of 4.5, a loss tangent of 0.002 and conductor-coating thickness of 35 μm. The design and simulation were performed by using CST Microwave Studio, in which the time-domain solver is specifically applied. Meanwhile, open boundary and waveguide ports were chosen to be used in the simulation. Then, the measurement was conducted by using a vector network analyzer (VNA).

## II. UWB POWER DIVIDER DESIGN

The configurations of the proposed power divider design are shown in Figs. 1 and 2. The design consists of two conductive layers: a top and bottom layer. The top layer incorporates the microstrip line with three ports, Port 1 (P1), Port 2 (P2), and Port 3 (P3), whereas the bottom layer consists of two rectangular-shaped slots underneath the microstrip lines. These microstrips and slots form two-section quarter-wave transformers. The rectangular-shaped microstrip line and slot are chosen to minimize fabrication errors since the fabrication is performed manually. Between each section of the quarter-wave transformer, two resistors ($R_1$ and $R_2$) are used to ensure that good isolation is achieved between the output ports, and any reflected power is dissipated at a wider frequency range. The width and length of the microstrip presented are denoted as $W_m$ and $L_m$, respectively. Meanwhile, the width and length of the slot are denoted as $W_s$ and $L_s$.

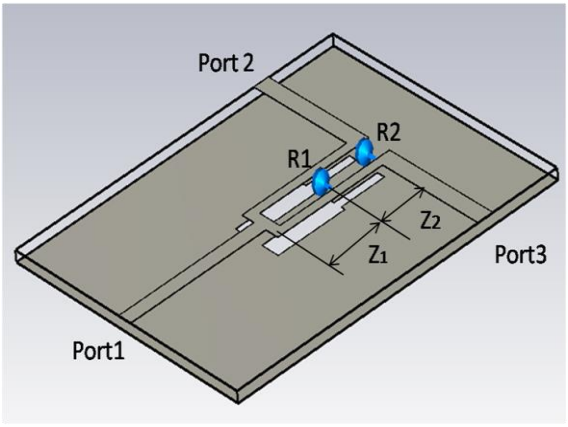


Fig. 1. The perspective view of the UWB two-section microstrip-slot power divider.

Figure 3 shows the equivalent circuit of the proposed designed power divider, which consists of impedance ($Z_0$), a capacitor (C), and a resistor (R) [4]. As observed from the figure, the circuit is divided into two output arms, in which each port has two fringe capacitances, $C_g$ located between the slot edges at the ground plane in the air region. The fringe capacitance, $C_g$ for the output arm P2 and P3, are denoted as $C_{g1}$ and $C_{g2}$, and $C_{g3}$ and $C_{g4}$, accordingly. Meanwhile, the parallel-plate capacitances, $C_{p1}$, $C_{p2}$, $C_{p3}$, $C_{p4}$, $C_{p5}$, and $C_{p6}$ denote the vertical capacitance between the top layer microstrip line and the ground plane.

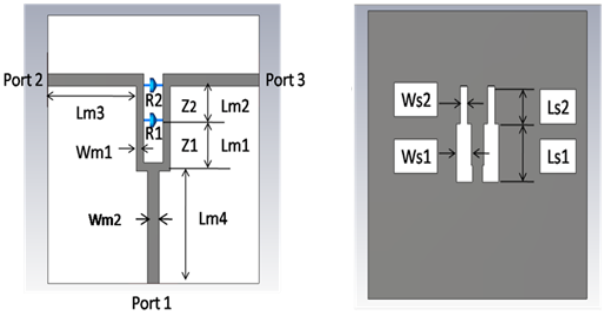


(a) (b)

Fig. 2. The detail configuration of UWB two-section microstrip-slot power: (a) top and (b) bottom view.

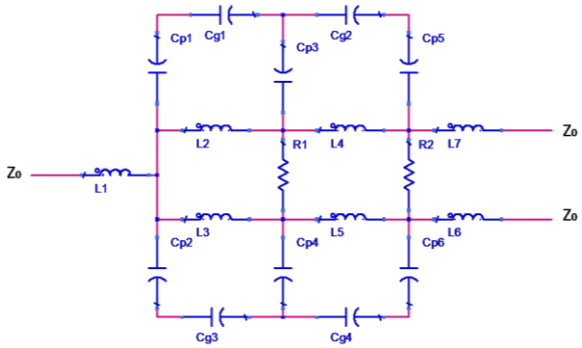


Fig. 3. The equivalent circuit of UWB two-section microstrip-slot power divider.

The characteristic impedances of the two-section quarter-wave transformers, $Z_1$ and $Z_2$, are determined through the binomial approach of the multi-section step impedance matching technique [4]. A binomial is chosen to obtain the maximal flat transmission coefficients of S21 and S31 across the designated frequency band. To calculate the value of $Z_1$ and $Z_2$, the value of $Z_L/Z_0$ must be known. The $Z_L/Z_0$ value can be computed through an even-mode analysis. As explained in [4], for the even-mode excitation, there is no current flow through the resistor $R_1$ and $R_2$. The value of $Z_0$ is assumed to be 50 Ω and the $Z_L$ to be $2Z_0$, and $Z_L/Z_0$ is equivalent to 2. Thus, the characteristic impedance of $Z_1$ and $Z_2$ can be computed from the respective equations (1) and (2) that redefined from the binomial multi-section step impedance matching equation in [4]:

$$\ln Z_1 = \ln Z_2 + 2^{-N} C_1^N \ln \frac{Z_L}{Z_0}, \tag{1}$$

$$\ln Z_2 = \ln Z_0 + 2^{-N} C_0^N \ln \frac{Z_L}{Z_0}, \tag{2}$$

where $N$ is the number of sections of the quarter-wave transformer. The binomial coefficients, $C_n^N$, can be obtained by using equation (3) [4]:

$$C_n^N = \frac{N!}{(N-n)!n!}, \tag{3}$$

where $n$ are 0 and 1. Note that, in this case, $N$ is 2 and the required binomial coefficients from equation (3) are $C_0^2 = 1$ and $C_1^2 = 2$. Therefore, the computed $Z_1$ and $Z_2$ from equations (1) and (2) are 84.09 Ω and 59.46 Ω, respectively.

The value of the resistors, $R_1$ and $R_2$, can then be obtained by performing the odd-mode analysis, wherein the odd-mode analysis, a null voltage is excited along the middle of the circuit. This excitation ensures that the two points on the mid-plane are grounded. By simplifying the circuit, the $R_1$ and $R_2$ can be calculated by using equation (4) and (5), accordingly [13]:

$$R_1 = \frac{2Z_1Z_2}{\sqrt{(Z_1+Z_2)(Z_1 - Z_2\cot^2\varphi)}}, \tag{4}$$

$$R_2 = \frac{4R_1Z_0(Z_1+Z_2)}{\sqrt{R_1(Z_1+Z_2) - 2Z_1}}, \tag{5}$$

where $\varphi$ can be obtained by using equation (6) [13]:

$$\varphi = \frac{\pi}{2}\left[1 - \frac{1}{\sqrt{2}}\left(\frac{f_2 - f_1}{f_2 + f_1}\right)\right], \tag{6}$$

where $f_1$ and $f_2$ are the start and stop frequencies of the designated band, respectively. Thus, the calculated values of the resistors $R_1$ and $R_2$ are 123.0 Ω and 201.91 Ω, accordingly.

As stated in the proposed design description, which is illustrated in Figs. 1 and 2, the two sections of the quarter-wave transformers with the characteristic impedance of $Z_1$ (84.09 Ω) and $Z_2$ (59.46 Ω) are used to achieve the bandwidth specification. This two-section of the quarter-wave is formed by a microstrip line with two rectangular slots underneath. This microstrip line with a slot underneath is named the microstrip-slot line, with the characteristic impedance of $Z_{m\text{-}s}$. The relationship between microstrip-slot impedance, $Z_{m\text{-}s}$ with the width of the slot, $W_s$ and microstrip line impedance, $Z_m$ can be expressed as in equation (7) [14]:

$$Z_{m-s} = 18.22W_s^2 + Z_m, \tag{7}$$

Table 1: Analysis of the effective length of the microstrip-slot quarter-wave sections 1 and 2 that correspond to the electrical length, $\theta = 90°$

| Effective Length of Microstrip-slot Quarter-wave Sections 1 and 2, $\theta = 90°$ | Parameters | | | |
|---|---|---|---|---|
| | Operating Frequency | Center Frequency, $f_c$ | Microstrip-slot Wavelength, $\lambda_{m\text{-}s}$ | Theoritical-slot Wavelength, $\lambda_S$ |
| 12.46 mm | 1 - 4 GHz | 2.5 GHz | 49.8 mm | 72.4 mm |
| 6.23 mm | 1 - 7 GHz | 4 GHz | 24.9 mm | 45.2 mm |
| 4.15 mm | 3 - 11 GHz | 7 GHz | 16.6 mm | 25.8 mm |
| 3.15 mm | 4 - 14 GHz | 9 GHz | 12.6 mm | 20.1 mm |
| 2.49 mm | 6 - 16 GHz | 11 GHz | 10.0 mm | 16.4 mm |

This equation is derived by using the completing square curve fitting method. However, the equation is only valid for microstrip-slot impedance, $Z_{m\text{-}s}$ ranging from 40 Ω to 100 Ω, dielectric permittivity, $\varepsilon_r$ between 2 and 5 and a substrate thickness, $h$ of 0.508 mm. In the case of this proposed power divider design, the characteristic impedance of the microstrip slots, $Z_{m\text{-}s}$ are $Z_1$ (84.09 Ω) and $Z_2$ (59.46 Ω), which correspond to sections 1 and 2 of the quarter-wave transformer. In contrast, the characteristic impedance of microstrip line, $Z_m$ is set to be 57.38 Ω that analogous to the microstrip width, $W_{m1}$ = 0.7 mm. According to these values of $Z_1$, $Z_2$ and $Z_m$, the computed slot widths ($W_{s1}$ and $W_{s2}$) of each section using equation (7) are 0.65 mm and 1.34 mm, respectively. Then, by using the obtained value of $W_{s1}$ and $W_{s2}$, the impedance of a slot can be determined by implementing equation (8) [15]:

$$Z_s = 73.6 - 2.15\varepsilon_r + \left(638.9 - 31.37\varepsilon_r\right)\left(W_s/h\right)^{0.6} \left(36.23\sqrt{\varepsilon_r^2 + 41} - 225\right)\frac{W_s/h}{W_s/h + 0.87\varepsilon_r - 2} + 0.51\left(\varepsilon_r + 2.12\right)\left(\frac{W_s}{h}\right)\ln\left(\frac{100h}{\lambda_0}\right) - 0.753\frac{\varepsilon_r\left(h/\lambda_0\right)}{\sqrt{W_s/h}}, \quad (8)$$

where $h$ and $\lambda_0$ are 0.508 mm and 46.15 mm, respectively. The formula in (8) is valid for the case of dielectric constant ($\varepsilon_r$) ranging from 3.8 to 9.8, $0.0015 < W_s/\lambda_0 < 0.075$ and $W_s/h > 1.67$. By applying equation (8), the slot impedance of each section is obtained to be 157.81 Ω and 125.83 Ω, respectively. In addition, the widths of the microstrip line at the top layer of the proposed design ($W_{m1}$ and $W_{m2}$) can be obtained using (9) by setting the values of the microstrip-line impedance ($Z$) as follows: the quarter-wave transformer ($Z_m$) is equivalent to 57.38 Ω, and characteristic impedance ($Z_0$) is equivalent to 50 Ω [4]:

$$\frac{W_{mi}}{h} = \frac{2}{\pi}\left[\frac{377\pi}{2Z\sqrt{\varepsilon_r}} - 1 - \ln\left(\frac{377\pi}{2Z\sqrt{\varepsilon_r}} - 1\right) + \frac{\varepsilon_r - 1}{2\varepsilon_r}\left\{\left(\frac{377\pi}{2Z\sqrt{\varepsilon_r}} - 1\right) + 0.39 - \frac{0.61}{\varepsilon_r}\right\}\right], \quad (9)$$

where $i$ = 1, 2. Therefore, the values of $W_{m1}$ and $W_{m2}$ obtained from equation (9) are 0.7 mm and 1.069 mm, respectively. Once the initial dimensions of the proposed two-section power divider have been obtained, the optimization is carried out using CST Microwave Studio. Due to the limitation of available commercial resistors in the market, $R_1$ and $R_2$ are set to be 130 Ω and 200 Ω, respectively, despite the calculated values from (4) and (5). The details of the optimized microstrip and slot width dimensions of the proposed design are given as follows: $W_{m1}$ = 0.7 mm, $W_{m2}$ = 1.07 mm, $W_{s1}$ = 0.65 mm, and $W_{s2}$ = 1.34 mm. The effective length of the two-section quarter-wave, $L_{m1}$, $L_{m2}$, $L_{s1}$ and $L_{s2}$ (which correspond to an electrical length of $\theta = 90°$), is according to the designated operating frequency. To obtain the length of the two-section quarter-wave transformer that formed by the microstrip-slot lines, a simple analysis was conducted, which is summarized in Table 1.

By having an optimized microstrip and slot widths that represent the characteristic impedances, the length of the microstrip-slot quarter-wave sections 1 and 2 are varied to observe the changes in the operating and center frequency. In any wideband microwave design, this center frequency is used as the designed frequency accordingly. Similar lengths of section 1 and 2 are considered, which concern the lengths of 12.46 mm, 6.23 mm, 4.15 mm, 3.15 mm and 2.49 mm. The increment of length, as expected, shifts the operating and center frequency to the higher range. Then, the microstrip-slot wavelength, $\lambda_{m\text{-}s}$ is compared to the theoretical slot wavelength, $\lambda_s$. In this analysis, slot wavelength, $\lambda_s$ is used, as its effective permittivity, $\varepsilon_{es}$, does not depend on the slot width and thickness of the substrate. This contrasts to the microstrip wavelength. The slot wavelength, $\lambda_s$ can be computed from (10) [2]:

$$\lambda_s = \frac{c}{f_c\sqrt{\varepsilon_{es}}}, \quad (10)$$

where $\varepsilon_{es} = (\varepsilon_r + 1)/2$ and the speed of light, $c = 3 \times 10^8$ ms$^{-1}$. Therefore, by referring to Table 1, microstrip-slot wavelength, $\lambda_{m\text{-}s}$ is approximately 0.62 of slot wavelength, $\lambda_s$. Consequently, the microstrip-slot effective permittivity,

$\varepsilon_{em\text{-}s}$ and microstrip-slot wavelength, $\lambda_{m\text{-}s}$ can be estimated from (11) and (12):

$$\varepsilon_{em-s} = 1.3(\varepsilon_r + 1), \tag{11}$$

$$\lambda_{m-s} = \frac{c}{f_c\sqrt{\varepsilon_{em-s}}}. \tag{12}$$

Hence, the initial sections 1 and 2 lengths of the microstrip-slot quarter-wave can be computed from (12). Then, the optimization is performed to obtain the optimal effective length. The optimized length dimensions are $L_{m1} = L_{m2} = L_{s1} = L_{s2} = 4.153$ mm, while the lengths to ports are $L_{m3} = 9.65$ mm and $L_{m4} = 10$ mm. The overall size of the proposed design after the optimization is 20 mm x 23 mm. When all the requirements are met, the design is fabricated and tested. The simulation and measurement results of the proposed design are discussed in the next section.

## III. RESULTS AND DISCUSSION

The prototype of the proposed UWB two-section power divider and its measurement setup using a VNA are presented in Fig. 4. Surface mount resistors, also known as SMD resistors, of 130 Ω and 200 Ω are used as $R_1$ and $R_2$ in this prototype, respectively. Referring to the measurement setup, the concerned ports are connected directly using special high-performance cables to the VNA, whilst other ports are terminated using an ultra wideband 50 Ω termination. Then, the obtained measurement results plotted in Figs. 5 and 6 are compared to the simulated ones and discussed.

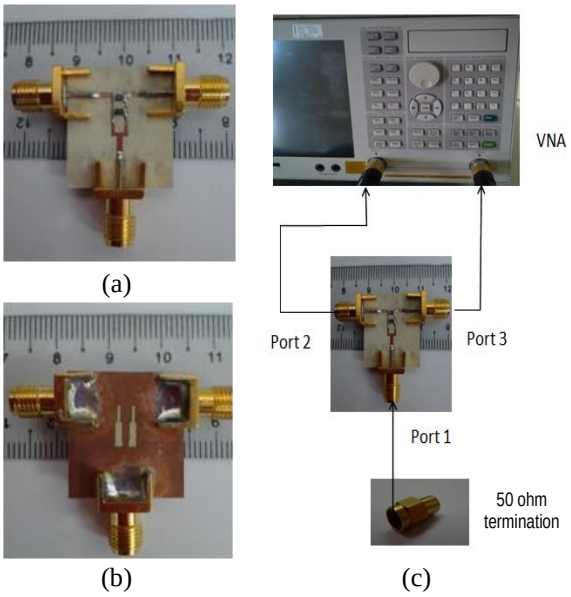


Fig. 4. (a) Top, (b) bottom view of the proposed UWB two-section power divider prototype, and (c) its configuration of measurement setup using a vector network analyzer (VNA).

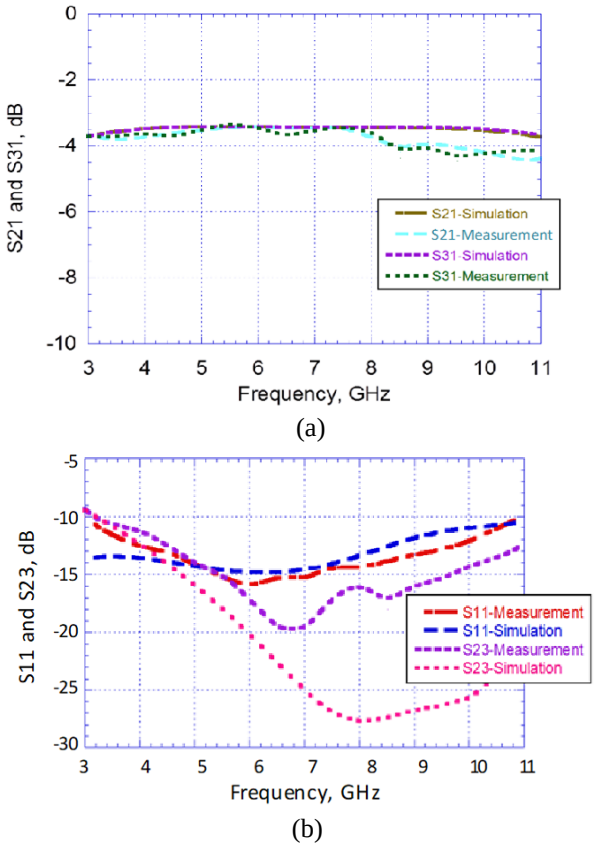


Fig. 5. Simulated and measured performance of the proposed UWB two-section power divider: (a) S21 and S31, and (b) S11 and S23.

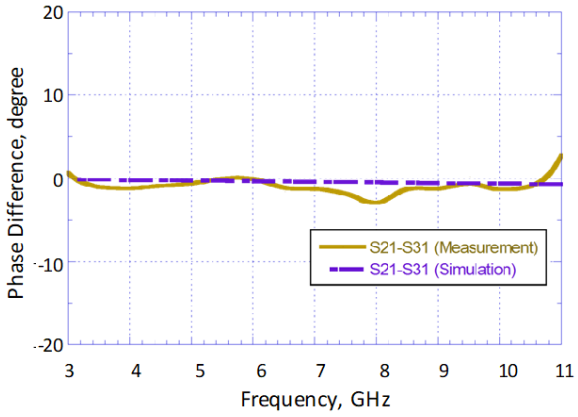


Fig. 6. The simulation and measurement results for phase difference between two output ports of the proposed two-section power divider.

The measurement and simulation performance levels of the transmission coefficients S21 and S31 are shown in Fig. 5 (a). It is noted that the results of S21 and S31 for simulation and measurement show almost

similar performance levels of -3.55 ± 0.15 dB and -3.8 ± 0.5 dB across 3 to 11 GHz, accordingly. Meanwhile, Fig. 5 (b) shows the simulated and measured results of the S11 and S23 of the proposed two-section power divider. By referring to the plotted simulation results, S11 and S23 are less than -10 dB for the whole band covering 3-11 GHz, whilst both the S11 and S23 results are lower than -10 dB for the same designated band. Furthermore, the simulation and measurement results for the phase difference between port 2 and 3 are depicted in Fig. 6. The plotted phase difference performance indicates the obtained simulation of 0° ± 0.2°. Meanwhile, the measurement result shows a comparable performance with a slight degradation of 0° ± 2° across 3 to 11 GHz. Then, the simulation and measurement results of S11, S21, S31, S23 and the phase difference between port 2 and 3 are summarized, as shown in Table 2.

Table 2: The comparison of the simulation and measurement results of the proposed two-section power divider

| Parameter | Simulated Performance | Measured Performance |
|---|---|---|
| S11 | ≤ -12 dB | ≤ -10 dB |
| S21 and S31 | -3.55 ± 0.15 dB | -3.8 ± 0.5 dB |
| S23 | ≤ -10 dB | ≤ -10 dB |
| Phase difference between Port 2 and 3 | 0° ± 0.2° | 0° ± 2° |

Referring to Table 2, it can be noted that both simulation and measurement results exhibit a good relative agreement even though there are slightly obvious differences due to the imperfect fabrication that was done in-house and additional losses contributed by the used connectors, terminations, and resistors. However, both simulation and measurement performances are acceptable and comply with the optimal power divider requirement across the designated UWB frequency range of 3-11 GHz.

Moreover, it is important to compare the proposed two-section microstrip-slot power divider to the conventional two-section power divider. The conventional power divider is designed at a center frequency of 6.85 GHz, which is similar to the proposed power divider. The comparisons are summarized in Table 3. In the conventional two-section power divider design, both section quarter-wave transformers have a length of 6.23 mm, which corresponds to a quarter-wavelength of microstrip $\lambda_m/4$ and an electrical length of $\theta$ of 90°. By implementing the rectangular-shaped slot underneath the microstrip line to form the quarter-wave transformer into the proposed power divider design, the length of both quarter-wave transformers can be reduced to 4.153 mm, which is equivalent to $\lambda_{m\text{-}s}/4$. This is due to the defections in the ground layer that disturb the current distribution in the ground plane and at the same time increase the effective inductance and capacitance of the microstrip line [16]. This contributes to reducing the size of the power divider circuit up to 23.33%. In addition to that, the bandwidth performance is improved up to 19.4% compared to the conventional two-section power divider.

Furthermore, as observed in Table 3, the conventional power divider design has a narrower microstrip line width at the section 1 quarter-wave transformer, which is 0.28 mm. To ensure that a very strong performance is achieved by the proposed power divider, precision fabrication is required. This very narrow microstrip line may lead to difficulty in the fabrication stage with a limited in-house facility. By introducing the rectangular-shaped slot at the ground plane underneath the microstrip line to form the quarter-wave transformer, a wider microstrip line of 0.7 mm can be used, which indirectly offers a better degree of fabrication tolerance. To maintain the impedance levels of each section of the quarter-wave transformer at 59.46 Ω and 84.09 Ω, each slot needs to have different widths, which are 0.65 mm and 1.34 mm, respectively. Thus, the microstrip-slot lines are obliged to have higher impedance due to the increment of its effective inductance and higher slow-wave factor compared to the conventional transmission lines [16].

Nonetheless, by concerning its size reduction and operating frequency, the proposed design is compared to the other related and published works in [2, 7, 10, 11]. By referring to Table 4, the proposed design has the broadest bandwidth of 9 GHz that covering 3-11 GHz with comparable small size as the design in [11]. The designs in [2, 6, 10] have larger size with narrower bandwidth. Therefore, the implementation of the microstrip-slot technique in the design has realized the goals of size reduction and bandwidth enhancement.

Table 3: The performance comparison between proposed and conventional two-section power divider

| Parameter | | Conventional Power Divider | Proposed Power Divider |
|---|---|---|---|
| Microstrip line width of quarter-wave transformer (mm) | Section 1 | 0.28 | 0.7 |
| | Section 2 | 0.65 | 0.7 |
| Length of quarter-wave transformer (mm) | Section 1 | 6.23 | 4.153 |
| | Section 2 | 6.23 | 4.153 |
| Size circuit ($mm^2$) | | 20 x 30 | 20 x 23 |
| Bandwidth (GHz) | | 3-9.7 | 3-11 |

Table 4: Comparison of the proposed design with the related and published works in [2, 7, 10, 11]

| Design | Technique | Size | % Claimed Size Reduction | Operating Frequency (GHz) |
|---|---|---|---|---|
| Proposed Design | Microstrip-slot | 20 mm x 23 mm | 23.33% | 3 - 11 (BW = 8) |
| [2] | Multilayer microstrip-slot | 24 mm x 40 mm | Not specified (larger) | 2 - 6 GHz (BW = 4) |
| [6] | Coupled-line | 6.33 mm × 22.1 mm | Not specified (smaller) | 2.4 |
| [10] | T-shaped step impedance transmission line | 56 mm × 56 mm | 53% | $f_1$ = 0.450 and $f_2 = k f_1$ , where ($k$ = 6.3, 6.7 and 7.3) |
| [11] | Small length transmission lines and open-circuited stubs | Not specified | Not specified (comparable) | 3.1 - 10.6 (BW = 7.5) |

*BW = Bandwidth

## IV. CONCLUSION

The design of a compact UWB two-section power divider by implementing the microstrip-slot technique was presented in this article. The microstrip-slot technique, which includes a rectangular-shaped slotline underneath each quarter-wave transformer section of two microstrip output arms, led to the reduction of the circuit size up to 23.33% compared to the conventional power divider. The power divider was fabricated and practically tested in the laboratory. The fabricated power divider showed good results in terms of return loss, isolation, transmission coefficients and phase difference between the output ports over a UWB frequency band range between 3 and 11 GHz. Additionally, a bandwidth improvement of 19.4% was demonstrated by this proposed power divider. Hence, this power divider is suitable to be used in many wireless applications that are in high demand nowadays, and that high demand is expected to continue in the future.

## ACKNOWLEDGMENT

This work was supported by Ministry of Education Malaysia (MOE) and Universiti Teknologi Malaysia (UTM) through Flagship, HiCoE, PRGS and FRGS Grant with the respective vote number of 03G41, 4J212, 4L684 and 5F048.

## REFERENCES

[1] C.-X. Wang, F. Haider, et al., "Cellular architecture and key technologies for 5G wireless communication networks," *IEEE Commun. Mag*., vol. 52, no. 2, pp. 122-130, Feb. 2014.

[2] N. Seman and S. N. A. M. Ghazali, "Design of multilayer microstrip-slot in-phase power divider with tuning stubs for wideband wireless communication applications," *Wirel. Pers. Commun.*, vol. 83, no. 4, pp. 2859-2867, Aug. 2015.

[3] D. N. A. Zaidel, S. K. A. Rahim, N. Seman, R. Dewan, and B. M. Sa'ad, "New ultra-wideband phase shifter design with performance improvement using a tapered line transmission line for a butler matrix UWB application," *Appl. Comput. Electromagn. Soc. J.*, vol. 29, no. 8, pp. 611-617, July 2014.

[4] D. M. Pozar, *Microwave Engineering*, 4th Edition, Wiley, New York, 2011.

[5] Q. Guo, Y. Ma, and J. Ju, "A novel broadband high-power combiner," *Asia-Pacific Microwave Conference*, Suzhou, pp. 3495-3498, Dec. 2005.

[6] D. Kang, Y.-H. Pang, and H.-H. Chen, "A compact wilkinson power divider/combiner with two-section coupled lines for harmonics suppression," *Asia-Pacific Microwave Conference*, Kaohsiung, pp. 995-997, Dec. 2012.

[7] S. Gruszczynski and K. Wincza, "Miniaturized broadband multisection coupled-line wilkinson power divider designed with the use of quasi-lumped element technique," *International Caribbean Conference on Devices, Circuits and Systems*, Playa del Carmen, pp. 1-4, Mar. 2012.

[8] H. Oraizi and A.-R. Sharifi, "Design and optimization of broadband asymmetrical multi-section Wilkinson power divider," *IEEE Trans. Microw. Theory Tech*., vol. 54, no. 5, pp. 2220-2231, May 2006.

[9] X.-P. Ou and Q.-X. Chu, "A modified two-section UWB Wilkinson power divider," *International Conference on Microwave and Millimeter Wave Technology*, Nanjing, pp. 1258-1260, Apr. 2008.

[10] A. Mahan, S. H. Sedighy, and M. Khalaj-Amirhosseini, "A compact dual-band planar 4-way power divider," *Appl. Comput. Electromagn. Soc. J.*, vol. 32, no. 3, pp. 243-248, Mar. 2017.

[11] S. Tsitsos, D. Efstathiou, P. Kyriazidis, and A. A. P. Gibson, "Design of an ultra wide-band power divider with harmonics suppression," *6th International Conference From Scientific Computing to Computational Engineering*, Athens, July 2014.

[12] M. F. Khajeh, S. A. Mirtaheri, and S. Chamaani, "Design and analysis of a band-notched UWB 1 to 4 Wilkinson power divider using symmetric defected ground structure," *European Conference on Antennas and Propagation*, Rome, pp. 860-864, Apr. 2011.
[13] S. B. Cohn, "A class of broadband three-port TEM-mode hybrids," *IEEE Trans. Microw. Theory Tech*., vol. 19, no. 2, pp. 110-116, Feb. 1968.
[14] K. H. Yusof, N. Seman, M. H. Jamaluddin, and D. N. A. Zaidel, "Characterization and formulation of microstrip-slot impedance with different thickness and relative permittivity," *Applied Mechanics and Materials*, vol. 781, pp. 53-56, Aug. 2015.
[15] R. Janaswamy and D. H. Schaubert, "Characteristic impedance of a wide slotline on low-permittivity substrates," *IEEE Trans. Microw. Theory Tech*., vol. 34, no. 8, pp. 900-902, Aug. 1986.
[16] L. G. Maloratsky, "Microstrip circuit with a modified ground plane," *High Frequency Electronic, Summit Technical Media*, pp. 38-47, 2009.

**Norhudah Seman** received the B.Eng. in Electrical Engineering (Telecommunications) degree from the Universiti Teknologi Malaysia, Johor, Malaysia, in 2003 and M.Eng. degree in RF/Microwave Communications from The University of Queensland, Brisbane, St. Lucia, Qld., Australia, in 2005. In September 2009, she completed her Ph.D. degree at The University of Queensland. Currently, she is an Associate Professor and Director (Communication Engineering) in School of Electrical Engineering and Research Fellow in HiCoE Wireless Communication Centre (WCC), Universiti Teknologi Malaysia. Her research interests concern the design of microwave/millimeterwave devices for biomedical and industrial applications, effects of electromagnetic field radiation including specific absorption rate (SAR), and mobile communications.

**Khairul Huda Yusof** received the diploma in Electrical Engineering (Telecomunication) and degree of B.Eng. in Electrical Engineering (Microelectronics) from Universiti Teknologi Malaysia in 2008 and 2011, respectively. Currently, she just completed her Ph.D. study in Electrical Engineering at Universiti Teknologi Malaysia, majoring in Telecomunication. She is now a Lecturer in Faculty of Engineering and Information Tehnology, MAHSA University, Malaysia.

**Mohd Haizal Jamaluddin** was born in Selangor, Malaysia. He received his Bachelor degree and Master degree in Electrical Engineering from Universiti Teknologi Malaysia (UTM), Malaysia in 2003 and 2006, respectively. He received the Doctoral degree in Signal Processing and Telecommunications from the University of Rennes 1, Rennes, France in 2010. He is currently an Associate Professor in UTM. His main field of interest is on antenna design especially on dielectric resonator antenna, reflect array antenna and lens antenna.

**Tharek Abd Rahman** is a Professor at Faculty of Electrical Engineering, Universiti Teknologi Malaysia (UTM). He obtained his B.Sc. in Electrical & Electronic Engineering from University of Strathclyde UK in 1979, M.Sc. in Communication Engineering from UMIST Manchester UK and Ph.D. in Mobile Radio Communication Engineering from University of Bristol, UK in 1988. He is the Director of Wireless Communication Centre (WCC), UTM. His research interests are radio propagation, antenna and RF design and indoors and outdoors wireless communication. He has also conducted various short courses related to mobile and satellite communication to the Telecommunication Industry and Government body since 1990. He has a teaching experience in the area of mobile radio, wireless communication system and satellite communication.